T. Picoli
https://orcid.org/0000-0002-4806-4973
C.M. Peter
https://orcid.org/0000-0001-7879-3299
M.G. Lopes
http://orcid.org/0000-0003-3955-445X
L.S. Barcelos
https://orcid.org/0000-0001-9235-9931
A.S. Varela Junior
https://orcid.org/0000-0003-4901-5118
C.D. Corcini
https://orcid.org/0000-0001-5683-7801
S.O. Hübner
https://orcid.org/0000-0003-0482-9599
G.A. Vargas
https://orcid.org/0000-0002-5126-3607
M. Lima
https://orcid.org/0000-0003-3102-1659
G. Fischer
https://orcid.org/0000-0002-3521-395X

Melittin-induced metabolic changes on the Madin-Darby Bovine Kidney cell line

[*Mudanças metabólicas induzidas por melitina em células da linhagem Madin-Darby Bovine Kidney*]

T. *Picoli*[1], C.M. *Peter*[1], M.G. *Lopes*[1], L.S. *Barcelos*[1], A.S. *Varela Júnior*[2], C.D. *Corcini*[1], S.O. *Hübner*[1], G.A. *Vargas*[1], M. *Lima*[1], G. *Fischer*[1*]

[1]Universidade Federal de Pelotas - Capão do Leão, RS
[2]Universidade Federal de Rio Grande - Rio Grande, RS

ABSTRACT

In this study, the toxic effects of melittin on Madin-Darby Bovine Kidney cells (MDBK) were analyzed with respect to mitochondrial functionality by reduction of MTT and flow cytometry, apoptosis potential, necrosis, oxygen reactive species (ROS) production, lipid peroxidation, and DNA fragmentation using flow cytometry and cell membrane destabilization by confocal microscopy. The toxicity presented dose-dependent characteristics and mitochondrial activity was inhibited by up to 78.24 ±3.59% (P<0.01, n = 6) in MDBK cells exposed to melittin (10μg/mL). Flow cytometry analysis revealed that melittin at 2μg/mL had the highest necrosis rate (P<0.05) for the cells. The lipoperoxidation of the membranes was also higher at 2μg/mL of melittin (P<0.05), which was further confirmed by the microphotographs obtained by confocal microscopy. The highest ROS production occurred when the cells were exposed to 2.5μg/mL melittin (P<0.05), and this concentration also increased DNA fragmentation (P<0.05). There was a significative and positive correlation between the lipoperoxidation of membranes with ROS (R=0.4158), mitochondrial functionality (R=0.4149), and apoptosis (R=0.4978). Thus, the oxidative stress generated by melittin culminates in the elevation of intracellular ROS that initiates a cascade of toxic events in MDBK cells.

Keywords: cytotoxicity, bee venom, apoptosis, necrosis, membrane

RESUMO

Neste estudo, os efeitos tóxicos da melitina em células Madin-Darby Bovine Kidney (MDBK) foram analisados quanto à funcionalidade mitocondrial, por redução de MTT e citometria de fluxo, potencial de apoptose, necrose, produção de espécies reativas de oxigênio (ROS), peroxidação lipídica e fragmentação de DNA, utilizando-se citometria de fluxo e desestabilização da membrana celular, por microscopia confocal. A toxicidade apresentou características dose-dependentes e a atividade mitocondrial foi inibida até 78,24±3,59% (P<0,01, n = 6) em células MDBK expostas à melitina (10μg/mL). Análises por citometria de fluxo revelaram que a melitina a 2μg/mL apresentou o maior índice necrótico celular (P<0,05). A maior lipoperoxidação de membranas também foi na concentração de 2μg/mL de melitina (P<0,05), o que foi posteriormente confirmado por microscopia confocal. A maior produção de ROS aconteceu quando as células foram expostas a 2,5μg/mL de melitina (P<0,05), e essa concentração também aumentou a fragmentação de DNA (P<0,05). Houve uma significativa correlação positiva entre a lipoperoxidação de membranas e a produção de ROS (R=0,4158), funcionalidade mitocondrial (R=0,4149) e apoptose (R=0,4978). Portanto, o estresse oxidativo gerado pela melitina culminou na elevação de ROS intracelular, que inicia uma cascata de eventos tóxicos nas células MDBK.

Palavras-chave: citotoxicidade, veneno de abelha, apoptose, necrose, membrana

INTRODUCTION

Apitoxin or bee venom is secreted by a specialized gland present in the worker bees and confined in a vesicle until the moment of stinging (Benton *et al.*, 1963). It is a complex mixture of nitrogenous compounds, containing several biologically active components, including enzymes, peptides, and biogenic amines, conferring a wide variety of allergic and pharmacological properties, such as anti-inflammatory, antimicrobial, and antitumor activities (Cardoso *et al.*, 2003; Abreu *et al.*, 2010).

Melittin is a highly active water-soluble toxic peptide, with only 26 amino acids in its conformation, present in the venom of honeybees and contributes to about 50% of its dry weight (Cruz-Landim and Abdalla, 2002). In the venous vesicle, melittin is arranged in a tetrameric form, which gives it a low toxicity (Cardoso *et al.*, 2003). However, after being released, it dissociates into a highly toxic monomeric form. In addition to it, phospholipase A2 is also present in the venom, which further amplifies the catalytic actions of melittin (Cardoso *et al.*, 2003; Koumanov *et al.*, 2003).

Melittin exerts a rapid cytolytic action by destabilizing the membranes and releasing the cytoplasmic content of various cell types (Dempsey, 1990). The hemolytic activity, being a characteristic biological effect, is used to detect the peptide in poisonous extracts (Tosteson *et al.*, 1985). Its lithic capacity is not only restricted to animal cells as it also exerts antibacterial and antifungal activities (Ashthana *et al.*, 2004). The objective of this study was to examine the effects of melittin in MDBK (Madin-Darby Bovine Kidney) cells by analysis of mitochondrial functionality, apoptosis potential, necrosis, ROS production, lipid peroxidation, DNA fragmentation and cell membrane destabilization.

MATERIALS AND METHODS

Melittin was acquired from Sigma-Aldrich Corp. (St. Louis, MO, USA). MDBK cells were obtained from the cell bank of the Laboratory of Virology and Immunology of the Veterinary School of the Federal University of Pelotas. Minimum essential medium with Eagle's salts (E-MEM, Sigma-Aldrich Corp., St. Louis, MO) supplemented with antibiotics penicillin (Sigma-Aldrich®, USA), streptomycin (Vetec®, Brazil), enrofloxacin (Bayer®, Brazil), and amphotericin B (Cristália®, Brazil) were used for cell culture in 96-well flat bottom polystyrene microplates (KASVI®, Brazil). Fetal bovine serum (FBS) was obtained from Gibco (Grand Island, NY, USA) and added to E-MEM (10%) when the need for cell multiplication. Dimethyl sulfoxide (DMSO), MTT (3- (4,5-dimethylthiazol-2yl)-2-5-diphenyl-2H-tetrazolate reagent), as well as other reagents used in flow cytometry and confocal microscopy, were commercially purchased from Sigma-Aldrich Corp. (St. Louis, MO, USA).

Melittin was dissolved in sterile E-MEM at a concentration of 1mg/mL and stored at −20°C. The different concentrations used in the experiments were made by diluting the stock solution in E-MEM. MDBK cells were maintained in a humid incubator at 37°C and 5% CO2 in cell culture bottles with E-MEM supplemented with 10% FBS. After the establishment of the monolayer and attaining approximately 80% confluency, the cells were transferred to 96 well plates (100μL/well) at a concentration of 3×10^4 cells/mL. After 24h in the incubator, the medium was carefully aspirated and melittin was added to the wells (100μL/well) at different concentrations (1 to 10μg/mL) in six replicates. All plates were incubated for 72h under the same conditions until the time of reading. MDBK cells maintained in E-MEM without exposure to melittin were used as controls.

The MTT reduction assay is used to determine cell viability through mitochondrial functionality (Mosmann, 1983). After an exposure to melittin, the supernatant was carefully aspirated and 50μL/well of 1mg/mL MTT solution was transferred. Then, the plates were incubated for another 4h under the same condition, the supernatant was removed and 100μL/well of DMSO was added to solubilize the generated formazan crystals. After 15min of constant stirring, the plates were read spectrophotometrically at 540nm. The 50% and 90% cytotoxic concentrations (CC) were calculated by the formula (AT/AC) × 100, where AT indicates the mean absorbance of the wells where cells received treatment and AC the mean of the control wells where cells did not receive melittin.

Arq. Bras. Med. Vet. Zootec., v.73, n.2, p.352-360, 2021

353

For flow cytometry, MDBK cells, cultured and exposed to melittin at different concentrations (1.0 to 2.5µg/mL) for 72h, were subjected to the specific reagent for each analysis and then trypsinized, resuspended in 100µL of E-MEM, and stored under refrigeration. The analysis was performed on Attune Acoustic Focusing Cytometer® (Applied Biosystems) and the results were evaluated using the Attune Cytometric Software version 2.1. Hoechst 33342 fluorescent probe (2mM) was used to separate MDBK (Hoechst positive) cells from the cell debris (negative hoechst). Cell populations were detected by a VL1 photomultiplier (450/40 filter). Twenty-thousand events were analyzed per sample with a flow rate of 50µL/s. For the detection of MDBK cell population, an FSC x SSC scatter plot was constructed.

About apoptosis/necrosis: after exposure to melittin, 2µL of fluorescein isothiocyanate-conjugated Annexin V antibody (FITC) was added and the cells were incubated for 1h. After, propidium iodide (PI, 50µg/mL) was added with further incubation for 10min (Masango *et al.*, 2015). The cells were removed from the plate and placed under refrigeration for readings in the flow cytometer. The viable cells were not labeled with fluorophores (FITC−, PI−), while apoptotic cells outsource phosphatidylserine which is recognized by Annexin V (FITC+, PI−), and the necrotic cells due to the ruptured nuclear membrane, show binding with PI (FITC−, PI+ and FITC+, PI+). The fluorescence was read through the photomultiplier BL3 (640 LP filter). The results were expressed as the percentage of the cell populations as calculated by the formula: (number of positive events/total number of events) × 100.

The Mitochondrial membrane potential (MMP) analysis was performed using rhodamine 123 fluorescent dye which concentrates on the active mitochondrial membranes when electrons are donated to the respiratory chain. After exposure of the MDBK cells to melittin, rhodamine 123 (100nM) was added into the plates and maintained for 1h, and the excess reagent was aspirated. The cells were analyzed for the fluorescence intensity emitted in more active (higher concentration of fluorescence, greater accumulation of rhodamine) and less active mitochondria (less fluorescence, less accumulation of rhodamine) (Gillan *et al.*, 2005). Rhodamine 123 fluorescence was read through the BL1 photomultiplier (530/30 filter).

The expressed data refer to the percentages of cells with low MMP, calculated by the formula: (number of cells with low MMP/total cell number) × 100.

In order to analyze the intracellular production of reactive oxygen species (ROS) the oxidation of the fluorescent dye 2', 7' dichlorofluorescein diacetate (H2DCF-DA) by the intracellular ROS was monitored. h2DCF-DA (1 mM) was added and retained for 1h to the cells after exposure to melittin. The fluorescence emitted was read by the photomultiplier BL1 (530/30 filter) and the data were expressed by the mean green fluorescence intensity ±standard error (Domínguez-Rebolledo *et al.*, 2011).

The lipid peroxidation of cell membranes was evaluated by the lipophilic fluorophore probe C11-BODIPY581/591, which is analogous to unsaturated fatty acids. The fluorescence of this probe changes after the lipidic peroxidation, as it emits red fluorescence when present on intact membranes but emits orange to green shades when membranes are attacked by oxidative radicals (Aitken *et al.*, 2007). C11-BODIPY581/591 was added to the cells for 2h, and it was aspirated and the concentrations of melittin were added. After incubation for 72h, the cells were trypsinized and subjected to read fluorescently. The results are expressed as the percentage of cell shaving peroxidized lipids at membranes. The results were obtained using the formula: (number of events with red fluorescence/total number of events) × 100.

For DNA fragmentation, after exposure to melittin, the cells were treated for 5min with the fluorescent probe acridine orange (AO) (Ojeda *et al.*, 1992). AO is inserted into the double-stranded DNA as a monomer but can also aggregate to single-stranded DNA. The monomeric AO bound to the intact DNA emits green fluorescence, while the aggregated AO emits orange to red fluorescence (Hoshi *et al.*, 1996). The results were expressed as percentages of cells with DNA fragmentation, calculated by the formula: (number of cells with orange fluorescence/total number of cells) × 100. The use of confocal microscopy: MDBK cells were grown on 0.13-mm thick glass cover plates in 24-well plates. After the establishment of the monolayer, the cells were exposed to different concentrations of melittin ranging from 1.0 to 2.5µg/mL for 72h.

354

Arq. Bras. Med. Vet. Zootec., **v.73, n.2, p.352-360, 2021**

The specific reagents were then added to the wells for the given time. The supernatants were aspirated, and the coverslips removed from the wells of the plate with the aid of forceps and placed on a slide for analysis under confocal microscopy (Inverted Spectral Laser Scanning Confocal Microscope, Leica, TCS SP8).

The destabilization of the plasma membranes was evaluated by the fluorescent and hydrophobic probe merocyanine-540 that presents tropism and intensely blends the membranes that have a high disorder of their components and that have lost their typical asymmetry (translocation of the phospholipids in lipid bilayer) (Langner and Hui, 1993). The analysis was combined with the addition of YO-PRO-1, a semipermeable probe that binds to cellular DNA, enabling a viability analysis associated with the membrane state (Thomas *et al*., 2006). For this analysis, after culturing the cells and exposing to melittin, merocyanine-540 (2.7 µM) and YO-PRO-1 (25 nM) were added to the wells for 10 min before visualizing under confocal microscope (the method was adapted from Peña *et al*., 2004). In addition, Hoechst 33342 was added in the same manner as already described. The intensity of red fluorescence emitted by merocyanine-540 indicates the levels of membrane destabilization and green fluorescence emitted by YO-PRO-1 indicates the cells with the labeled DNA due to the high degree of membrane disorganization.

The data obtained by the MTT assay are represented by the mean ± standard deviation (SD). Analysis of variance (ANOVA, Tukey's test) was performed to evaluate the differences between the treatment groups and the control group. The flow cytometry data were subjected to analysis of variance (ANOVA, LSD test) for comparison of the groups. Pearson's correlations were performed to evaluate associations between the analyzed variables. In all cases, Statistix statistical software version 10.0® was used and significant results were considered when P<0.05.

RESULTS AND DISCUSSION

The MTT assay revealed a decrease in mitochondrial functionality of up to 78.24 ±3.59% (P<0.01, n = 6) for MDBK cells at a concentration of 10µg/mL of melittin in a dose-dependent manner (Table 1). The lowest concentrations (1 and 2µg/mL) showed the highest mitochondrial

activity rates (0.97% ±0.04% and 0.94% ±0.03%, respectively) and did not differ from the control, whereas all other concentrations of melittin decreased the mitochondrial activity of exposed cells (P<0.05, n = 6).

Table 1. Mitochondrial function of MDBK cells exposed to melittin and assessed by MTT reduction assay

Melittin	Mitochondrial Functionality (% ±SD, n=6)
10.0 µg/mL	21.76 ±3.59**
9.0 µg/mL	25.31 ±2.17**
8.0 µg/mL	28.84 ±1.45**
7.0 µg/mL	28.97 ±2.54**
6.0 µg/mL	29.50 ±1.77**
5.0 µg/mL	28.97 ±1.41**
4.0 µg/mL	30.23 ±2.06**
3.0 µg/mL	41.68 ±1.42*
2.0 µg/mL	99.03 ±0.04
1.0 µg/mL	99.06 ±0.03

* P<0.05; ** P<0.01. Indicating a statistical difference compared to the control (100% mitochondrial functionality); SD: Standard Deviation.

The cytotoxicity of melittin in a dose-dependent manner as described herein, corroborate previous reports (Pratt *et al*., 2005; Cerne *et al*., 2013). The 50% CC of melittin for MDBK cells was 2.32µg/mL and the 90% CC was 2.76µg/mL. The MTT assay measures cell viability as assessed by the mitochondrial functionality. In this context, an active state of mitochondria does not always reflect cellular health, since their activity is also increased in cases of cellular injury. This organelle may act as a pro-apoptotic signal after a damage to its membrane with consequent permeabilization and release of pro-apoptotic molecules present therein (Grivicich *et al*., 2007). Our results are in agreement with previous findings reported by Zhou *et al*. (2013), who described only 6.46% ±1.83% (P<0.05, n = 6) in hepG2 cells exposed to melittin at 10.0µg/mL. Results obtained by flow cytometry analysis indicated damage to cells, which were not detectable by the MTT test, as the latter estimates cell viability only by mitochondrial activity. The rates of apoptosis and necrosis, as analyzed by flow cytometry, are given in Figure 1. Other physiological changes in the cells were demonstrated by flow cytometry analysis (Table 2). When the cells were exposed to higher concentrations of melittin, the necrotic cell rates were increased.

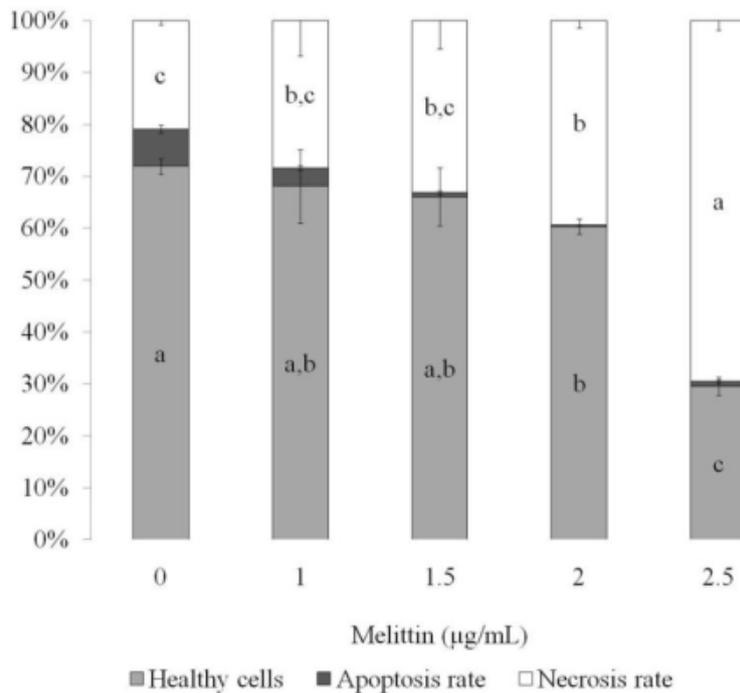*Arq. Bras. Med. Vet. Zootec.*, v.73, n.2, p.352-360, 2021

355

Figure 1. Flow cytometry analysis of normal MDBK cells and during apoptosis and necrosis after an exposure to melittin at different concentrations for 72h. Different letters in the same cell population indicate statistical difference by the LSD test (P<0.05).

Table 2. Quantification of reactive oxygen species (ROS), percentage of membrane lipid peroxidation (LPO), DNA fragmentation (DNAfrag), and mitochondrial membrane potential (MMP) of MDBK (Madin-Darby Bovine Kidney) cells exposed to melittin, as determined by flow cytometry

		LPO (% ±SE)	ROS (LI ±SE)	DNAfrag (% ±SE)	MMP (% ±SE)
Control		67.96 ±1.11 a	17237 ±5017.3 b	2.57 ±0.77 b	16.07 ±0.69 b
	1	69.72 ±1.34 ab	28009 ±11155 b	0.6 ±0.06 c	16.9 ±0.23 ab
melittin	1.5	70.44 ±1.31 ab	26580 ±17043 b	2.13 ±0.43 b	16.87 ±0.52 ab
(µg/mL)	2	73.14 ±0.77 c	21859 ±2097.1 b	3.21 ±0.69 b	17.8 ±0.67 a
	2.5	69.85 ±2.27 b	43360 ±12289 a	4.8 ±0.4 a	16.6 ±0.56 ab

Different letters in the same column indicate statistical difference by the LSD test (P<0.05). SE: Standard Error; LI: Luminescence Intensity.

Regarding the cell necrosis, the control cells showed 20.9% ±0.8% of cellular necrosis. Zhou *et al.* (2013), by a flow cytometric analysis after an exposure of hepG2 cells (derived from hepatocarcinoma) to melittin (0, 1, 2, and 5µg/mL), found necrosis rates of 0%, 6.8%, 1.6%, and 0.8%, respectively. The treatments with 1 and 1.5µg/mL of melittin did not show difference from the control. However, there was statistically significant difference (P<0.05) at the highest concentrations of melittin, as 39.4% ±1.5% necrotic cells were seen at 2µg/mL of melittin (non-toxic to MTT reduction) and 69.7% ±1.8% at 2.5µg/mL of melittin. Zhou *et al.* (2013) results

demonstrated lower rates of cellular necrosis than those found in this study, but it should be considered that in their study, the necrosis rate of the control group was subtracted from all other groups. Furthermore, the cells studied by these authors are derived from hepatocarcinoma and were exposed to melittin for 24h while in our study MDBK cells were exposed to melittin for 72h.

DNA fragmentation was also evaluated by flow cytometry which revealed that MDBK cells exposed to 2.5µg/mL of melittin (4.8% ±0.4%) showed the maximum impact of melittin toxicity.

The difference was statistically significant when compared to the cell control (2.57% ±0.77%) (P<0.05) (Table B.2); however, interestingly, the DNA fragmentation rate (0.6% ±0.06%) at 1μg/mL of melittin was lower than cell control. An exposure to melittin caused oxidative stress in MDBK cells by increasing the intracellular production of ROS. The cells exposed to 2.5μg/mL of melittin presented a mean of 43360 ±12289 LI and differed statistically (P<0.05) from the control (17237 ±5017.3) and from other concentrations. The elevated level of intracellular ROS indicates a biochemical imbalance to the point of altering the natural balance between pro-oxidants and antioxidants. The changes in the redox balance of biological systems such as cells, organelles, and tissues can cause oxidative stress (Schafer and Buettner, 2001).

There were no other changes in mitochondrial membrane potential (MMP) patterns. All treatments resulted in an increase in MMP of MDBK cells, but there was a statistical difference (P<0.05) between control (16.07%±0.69%) and treatment with 2μg/mL (17.8%±0.67%). Also, LPO showed a significant correlation with MMP (r = 0.4149, P<0.05), suggesting an increase in mitochondrial functions in an attempt to revert the stress caused to the cells by melittin. The rate of apoptosis could still be influenced by the release of pro-apoptotic mitochondrial messengers but there was a low and non-significant correlation between MMP and apoptosis (r = 0.1238, P>0.05).

The action of melittin occurs mainly on phospholipid membranes of the cells as described by Terwilliger *et al*. (1982), causing permeabilization, artificial pore formation, disruption, and lysis (Lee *et al*., 2008; Zhang *et al*., 2011). The mechanisms of action proposed on the membranes were explained by a "barrel model" and "carpet model". In the first model, the aggregates of melittin are perpendicularly formed on the surface of the membrane, resulting in membrane rupture in the form of toroidal pores (or in the form of a barrel). In the carpet model, melittin is distributed on the surface of the membrane in a parallel fashion, disorganizing the lipid bilayer and causes permeabilization (Bechinger, 1999; Gordon-Grossman *et al*., 2012). Both proposed models suggest the formation of pores or permeabilization of the membranes, explaining the appearance of necrotic cells after exposure to melittin and amplified in a proportion to the concentration of it.

While analyzing the destabilization of the phospholipid membranes of MDBK cells exposed to melittin with the aid of confocal microscopy, the microphotographs revealed greater destabilization concomitant with the increase in the concentration of melittin (Figure 2), according to the results obtained by flow cytometric analysis for lipid peroxidation.

As shown in Table 2, the increase in the LPO of membranes was directly proportional to the concentration of melittin, which showed statistically significant difference from the control (P<0.05). In addition to the already known mechanisms of action of melittin directly on the lipid membranes (barrel and carpet models), the LPO may also be caused by ahigh production intracellular ROS. Lipid peroxidation is a chain reaction that starts by attacking lipids by an ROS that has sufficient reactivity to sequester a hydrogen atom from a methylene (CH-2) group. The termination of this process is marked by the propagation of lipid and peroxyl radicals produced until they destroy themselves (Ferreira and Matsubara, 1997). Basically, LPO involves incorporating molecular oxygen into a fatty acid to produce a lipid hydroperoxide as the starting primary product. The LPO process occurs in several stages and with numerous possibilities of chemical reactions, which makes it difficult to understand and evaluate the process as a whole (Lima and Abdalla, 2001).
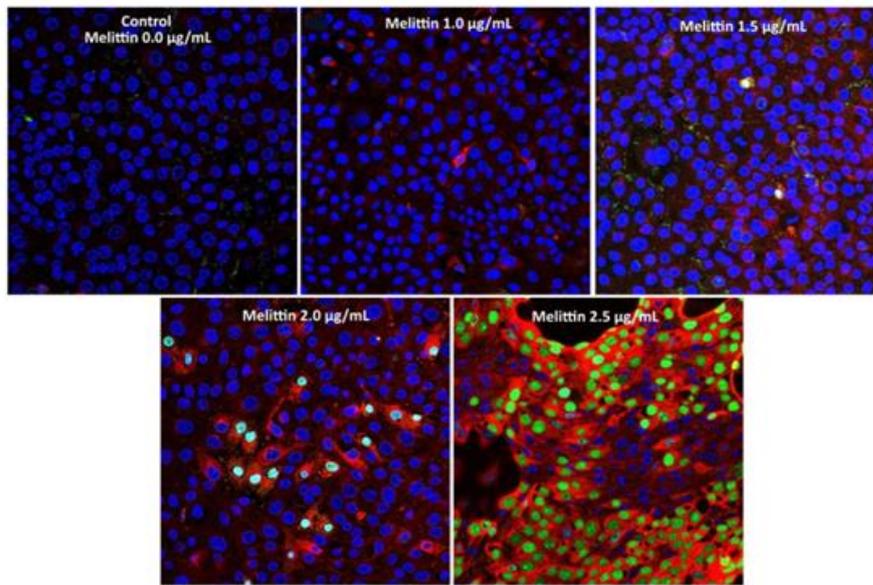
Figure 2. Membrane destabilization. Microphotographs were obtained by confocal microscopy of MDBK cells exposed to melittin (0, 1.0, 1.5, 2.0 and 2.5µg/mL) for 72h.

An exposure to melittin elevates cellular metabolism. The increase in the concentration of melittin resulted in a concomitant increase in the levels of ROS, LPO, MMP, and cellular necrosis but the rate of apoptosis was decreased, which was inversely proportional to the rate of necrosis ($r = -0.7049$, $P<0.001$). The free radicals attack the cell itself and the lipids in the cell membrane are peroxidized, which explains the correlation between ROS and LPO ($r = 0.4158$, $P<0.05$). The peroxidation of lipids resulted in the destabilization of membranes, as shown in Figure 2, making possible the cyclization of phosphatidylserine, characterizing an apoptotic process. This mechanism explains the observed correlation between LPO and the rate of apoptosis ($r = 0.4978$, $p<0.05$). The correlations between the analyzed variables are shown in Figure3, which may contribute for the elucidation on the mechanism of action of melittin on MDBK cells.
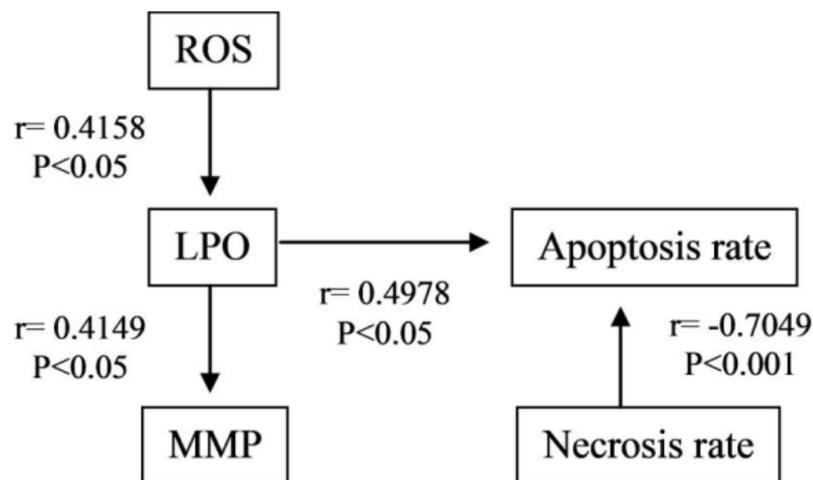

Figure 3. Pearson's correlations between the cellular function parameters as evaluated in MDBK cells exposed to melittin for 72h.

CONCLUSION

In this study, different analyses were performed in order to elucidate the action mechanisms of melittin toxicity on MDBK cells. The toxicity presented dose-dependent characteristics. Melittin at 2μg/mL had the highest necrosis rate for the cells and lipoperoxidation of the membranes. The highest ROS production occurred when the cells were exposed to 2.5μg/mL melittin, and this concentration also increased DNA fragmentation. There was a significative and positive correlation between the lipoperoxidation of membranes with ROS, mitochondrial functionality and apoptosis.

ACKNOWLEDGEMENTS

REFERENCES

ABREU, R.M.; MORAES, R.L.S.; CAMARGO-MATHIAS, M.I. Biochemichal and cytochemical studies of enzymatic activity the venom glands of workers of honey bee Apis mellifera L. (Hymenoptera, Apidae). *Micron*, v.41, p.172-175, 2010.

AITKEN, R.J.; WINGATE, J.K.; IULIIS, G.N.; MCLAUGHLIN, E.A. Analysis of lipid peroxidation inhuman spermatozoa using BODIPY C11. *Mol .Hum. Reprod.*, v.13, p.203-211, 2007.

ASHTHANA, N.; YADAV, S.P.; GHOSH, J.K. Dissection on antibacterial and toxic activity of mellitin: a leucine zipper motif plays a crucial role in determining itshemolytic activity bus not antibacterial activity. *J. Biol. Chem.*, v.279, p.55042-55050, 2004.

BECHINGER, B. The structure, dynamics and orientation of antimicrobial peptides in membranes by multidimensional solid-state NMR spectroscopy. *Biochim. Biophys. Acta*, v.1462, p.157-183, 1999.

BENTON, A.W.; MORSE, R.A.; STEWART, J.D. Venom colletion fromhoney bees. *Science*, v.142, p.228-230, 1963.

CARDOSO, J.L.C.; FRANÇA, F.O.S.; WEN, F.H. *et al*. *Animais peconhentos no Brasil*: biologia clínica e terapêutica dos acidentes. São Paulo: Sarvier/Fapesp, 2003. 468p.

CERNE, K.; ERMAN, A.; VERANIC, P. Analysis of cytotoxicity of melittin on adherent culture ofhuman endothelial cells reveals advantage of fluorescence microscopy over flow cytometry andhaemocytometer assay. *Protoplasma*, v.250, p.1131-1137, 2013.

CRUZ-LANDIM, C.; ABDALLA, F.C. *Glândulas exócrinas das abelhas*. Ribeirão Preto: FUNPEC, 2002. 182p.

DEMPSEY, C.E. The actions of melittin on membranes. *Biochim. Biophys. Acta*, v.1031, p.143-161, 1990.

DOMÍNGUEZ-REBOLLEDO, A.E.; MARTÍNEZ-PASTOR, F.; BISBAL, A.F. *et al*. Response of thawed epididymal red deer spermatozoa to increasing concentrations of hydrogen peroxide, and importance of individual male variability. *Reprod. Domest. Anim.*, v.46, p.393-403, 2011.

FERREIRA, A.L.A.; MATSUBARA, L.S. Radicais livres: conceitos, doenças relacionadas, sistema de defesa e estresse oxidativo. *Rev. Assoc. Med. Bras.*, v.43, p.61-68, 1997.

GILLAN, L.; EVANS, G.; MAXWELL, W.M. Flow cytometric evaluation of sperm parameters in relation to fertility potential. *Theriogenology*, v.63, p.445-457, 2005.

GORDON-GROSSMAN, M.; ZIMMERMANN, H.; WOLF, S.G. *et al*. Investigation of model membrane disruption mechanism by melittin using pulse electron paramagnetic resonance spectroscopy and cryogenic transmission electron microscopy. *J. Physiol. Chem. B.*, v.116, p.179-188, 2012.

GRIVICICH, I.; REGNER, A.; ROCHA, A.B. Morte celular por apoptose. *Rev. Bras. Cancerol.*, v.53, p.335-343, 2007.

HOSHI, K.; KATAYOSE, K.; YANAGIDA, K. *et al*. The relationship between acridine orange fluorescence of sperm nuclei and the fertilizing ability of human sperm. *Fertil. Steril.*, v.66, p.634-639, 1996.

Arq. Bras. Med. Vet. Zootec., v.73, n.2, p.352-360, 2021

359

KOUMANOV, K.; MOMCHILOVA, A.; WOLF, C. Bimodal regulatory effect of melittin and phospholipase A2-activating protein onhuman type II secretory phospholipase A2. *Cell Biol. Int.*, v.27, p.871-877, 2003.

LANGNER, M.; HUI, S.W. Merocyanine interaction with phosphatidylcholine bilayers. *Biochim. Biophys. Acta*, v.1149, p.175-179, 1993.

LEE, M.T.; HUNG, W.C.; CHEN, F.Y.; HUANG, H.W. Mechanism and kinetics of pore formation in membranes by water-soluble amphipathic peptides. *Proc. Natl. Acad. Sci.*, v.105, p.5087-5092, 2008.

LIMA, E.S.; ABDALLA, D.S.P. Peroxidação lipídica: mecanismos e avaliação em amostras biológicas. *Rev. Bras. Ciên. Farm.*, v.37, p.293-303, 2001.

MASANGO, M.G.; ELLIS, C.E.; BOTHA, C.J. Characterization of cell death caused by diplodiatoxin and dipmatol, toxic metabolites of Stenocarpellamaydis. *Toxicon*, v.102, p.14-24, 2015.

MOSMANN, T. Rapid colorimetric assay for cellular growth and survival: application to proliferation and cytotoxicity assays. *J. Immunol. Methods*, v.65, p.55-63, 1983.

OJEDA, F.; GUARDA, M.J.; MALDONADO, C.; FOLCH, H. A flow-cytometric method to study DNA fragmentation in lymphocytes. *J. Immunol. Methods*, v.152, p.171-176, 1992.

PEÑA, F.J.; JOHANNISSON, A.; WALLGREN, M.; MARTINEZ, H.R. Antioxidant supplementation of boar spermatozoa from different fractions of the ejaculate improves cryopreservation: changes in sperm membrane lipid architecture. *Zygote*, v.12, p.117-124, 2004.

PRATT, J.P.; RAVNIE, D.J.; JIANG, X. *et al.* Melittin-induced membrane permeability: a nonosmotic mechanism of cell death. *In Vitro Cell. Dev. Biol. Anim.*, v.41, p.349-355, 2005.

SCHAFER, F.Q.; BUETTNER, G.R. Redox environment of the cell as viewed through the redox state of the glutathione disulfide/glutathione couple. *Free Radic. Biol. Med.*, v.30, p.1191-1212, 2001.

TERWILLIGER, T.C.; WEISSMAN, L.; EISENBERG, D. The structure of melittin in the form I crystals and its implication for melittin's lytic and surface activities. *Biophys. J.*, v.37, p.353-361, 1982.

THOMAS, A.D.; MEYERS, S.A.; BALL, B.A. Capacitation-like changes in equine spermatozoa following cryopreservation. *Theriogenology*, v.65, p.1531-1550, 2006.

TOSTESON, M.T.; HOLMES, S.J.; RAZIN, M.; TOSTESON, D.C. Melittin lysis of red cells. *J. Membr. Biol.*, v.87, p.35-44, 1985.

ZHANG, N.Z.; QI, J.X.; FENG, S.J. *et al.* Crystal structure of swine majorhistocompatibility complex class I SLA-1*0401 and identification of 2009 pandemic swine-origin influenza Ah1N1 virus cytotoxic t lymphocyte epitope peptides. *J. Virol.*, v.85, p.11709-11724, 2011.

ZHOU, J.; QI, Y.; DIAO, Q. *et al.* Cytotoxicity of melittin and apamin inhumanhepatic L02 andhepG2 cells in vitro. *J. Toxicol. Toxin. Rev.*, v.32, p.60-67, 2013.

360

Arq. Bras. Med. Vet. Zootec., v.73, n.2, p.352-360, 2021